

# Closed strings in a class of pp-wave spacetimes and the memory effect

Ayan Dey and Sayan Kar\*

*Department of Physics, Indian Institute of Technology, Kharagpur 721 302, India*

## Abstract

We study closed string evolution in the pp-wave spacetime assuming different pulse shapes (square and sech-squared) in the exact gravitational wave metric. It is shown that the shape of a circular closed string deforms permanently, after the pulse has departed. The worldsheet geometry also displays characteristic permanent changes caused by the gravitational wave pulse. The above effects collectively demonstrate features akin to what is known as ‘memory’ in gravitational wave physics.

arXiv:2407.10095v3 [gr-qc] 14 Oct 2024

---

\* [ayan11@kgpian.iitkgp.ac.in](mailto:ayan11@kgpian.iitkgp.ac.in), [sayan@phy.iitkgp.ac.in](mailto:sayan@phy.iitkgp.ac.in)

## I. INTRODUCTION

In studies on the physics of gravitational waves, the gravitational wave memory effect is often illustrated by considering the change of shape of a ring of particles when it encounters a gravitational wave pulse for a short duration of time [1, 2]. For example, if the circular shape of the ring of particles gets *permanently* deformed to an elliptical (or any other) shape, we say that the pulse has ‘memory’. On the other hand, if the deformation is not permanent and the ring reverts back to its circular shape we say that the pulse has ‘no memory’. Such a visually appealing picture is very helpful in providing an elegant way of appreciating what ‘memory’ really means (see Figure 1). This illustrative example is by no means a toy example—in fact it has in it the very basic idea of ‘permanent change’ which lies at the heart of all ways of defining memory.

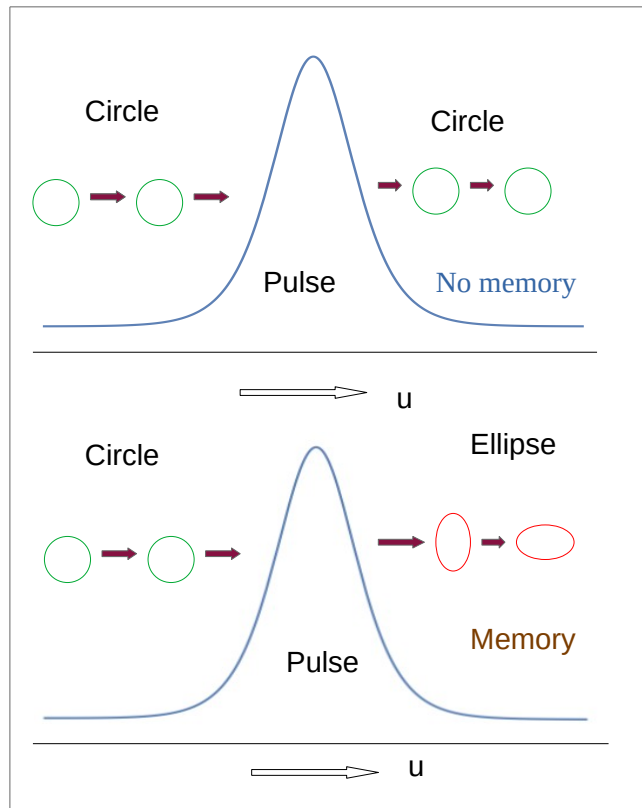


Figure. 1: Qualitative idea of memory for a ring of particles experiencing a GW pulse.

If we smoothen out the so-called ‘ring of particles’ what we get is a closed string. Right now, we are yet to state whether we are dealing with fundamental strings or cosmic strings. In our way of looking at the problem, it could be anything – in fact, even a macroscopic, elastic, circular string. The simplest description of such a string, in a relativistic setting, uses the Nambu–Goto area action, the ensuing equations of motion, their solutions and corresponding physical consequences [3]. The string configuration  $x^i(\tau, \sigma)$ , where  $\tau$  and  $\sigma$  are the worldsheet surface coordinates, is an extremal (minimal) surface in a background spacetime with a metric  $g_{ij}(x^k)$ . It is given mathematically through solutions of the Nambu–Goto equations of motion and constraints. For closed strings, we have the condition–  $x^i(\tau, \sigma) = x^i(\tau, \sigma + 2\pi)$ . If such a closed string encounters a gravitational wave pulse what happens to its circular shape? Do we see a permanent change at later times, i.e. much after the pulse has disappeared? We intend to answer such a question in our work here.

How do we model the gravitational wave pulse ? It is possible to use the perturbative approach and use a form of  $h_{ij}$  which is pulse-like. This may be observationally more relevant. However, here we would like to restrict ourselves to the purely theoretical domain and consider a pp-wave geometry (an exact gravitational wave solution of the vacuum Einstein equations) [4],[5]. In such a geometry we have a free function which we may choose appropriately, in order to represent a specific pulse shape. Hence, we would be studying the evolution of closed strings in a pp-wave spacetime through which we will try to arrive at what is conventionally known as the ‘memory’ effect.

Studies on strings in pp-wave spacetimes are not new. Past research in this subject area can be found in several older articles [6–9]. Very recently, Liška and von Unge [10] have revisited the topic in an interesting paper which originally motivated us to pursue the work reported here. On the other hand, string memory has been discussed in the recent past in [11] and stringy corrections to electromagnetic memory effects in [12].

In general, gravitational wave memory has been a topic of active research interest over the last few years. The prospect of detection of memory in future detectors has greatly influenced such studies [13], [14] (see [15], [16] and [17] for recent updates). The origins of the idea of GW memory in linearised gravity are in the papers by Zel’dovich, Polnarev [18] and Braginsky, Grishchuk [19] (the term ‘memory’ in the context of gravitational waves was introduced in this paper). Subsequently, Christodoulou[20], using full GR, showed how gravitational waves travelling to null infinity can give rise to a contribution to memory. Later,

it was [claimed](#) in [21], using gauge invariant observables, that for linearized gravity with a null matter stress-energy tensor, one recovers an effect analogous to nonlinear memory, though this does not show that nonlinear memory arises in the linearized theory. As emphasized in [21] one still needs to go to quadratic order in general relativity to see nonlinear memory. Related work on ‘ordinary’ and ‘null’ memory (as defined in [21]) are available in [22–25]. On the other hand, an interesting theoretical link involving the memory effects, the Bondi-Metzner-Sachs (BMS) symmetries and soft theorems has been shown to exist and explored in [26, 27]. Memory in pp-wave and related spacetimes have been extensively studied in a large number of papers [28–38] where diverse aspects of displacement and velocity memory have been thoroughly analysed. A novel ‘displacement within velocity memory’ which happens for a specific choice of the wave parameters, has recently been reported in [39]. A more general approach which aims at defining various ‘persistent gravitational wave observables’ has been pursued by Flanagan, Nichols, Grant and Harte in a series of papers [40–43]. An idea named as  $\mathcal{B}$ -memory (related to the  $\mathcal{B}$  tensor which encodes the behaviour of the gradient of the geodesic velocity field) appeared in the work in [44] and was followed up in [33]. Other work on diverse aspects of memory may be found in [45–47]. The review article [1] and the lecture by Favata [2] chronicles the history till 2010. A very recent review on the memory effect, asymptotic symmetries and its connections with numerical relativity is available in [48].

Our article is organised as follows. In the next section (II), we write down the string equations of motion and constraints in a pp-wave spacetime, using the conformal gauge. Thereafter, in III, assuming a square pulse gravitational wave, we obtain solutions at late times, assuming a circular closed string configuration, before the arrival of the pulse. In this way, via the permanent change of shape of the closed string we are able to arrive at a memory effect. We also do a similar analysis for a continuous pulse shape (the sech-squared pulse). In IV, we discuss some features such as the behaviour of the induced metric, the worldsheet Ricci scalar and the worldsheet geometry as an embedding. Finally in Section V we present our conclusions.

## II. STRINGS IN PP-WAVE SPACETIMES

Let us begin by first recalling the string equations of motion and constraints which follow from the variation (w.r.t.  $x^i$ ) of the Nambu–Goto area action ( $S_{NG} = -T_0 \int d\tau d\sigma \sqrt{-\gamma}$ ,  $\gamma$  being the determinant of the induced metric  $\gamma_{ab} = g_{ij} \partial_a x^i \partial_b x^j$  with  $a, b \dots$  being the world-sheet indices  $\tau, \sigma$  and  $T_0$ , the string tension). The equations of motion are:

$$\ddot{x}^i - x^{i''} + \Gamma_{jk}^i \left( \dot{x}^j \dot{x}^k - x^{j'} x^{k'} \right) = 0 \quad (1)$$

and the constraints (conformal gauge) are:

$$g_{ij} \dot{x}^i x^{j'} = 0 \quad (2)$$

$$g_{ij} \dot{x}^i \dot{x}^j + g_{ij} x^{i'} x^{j'} = 0 \quad (3)$$

where the dot and prime denote differentiation w.r.t.  $\tau$  and  $\sigma$ , respectively. The two constraints ensure that the induced metric  $\gamma_{ab}$  (as defined above) is diagonal. We will need to solve the Eqn. (1) written in a background geometry with metric  $g_{ij}$ , subject to the constraints in (2) and (3).

The plane parallel (*pp*) wave geometry which is a vacuum solution of the Einstein equations is given by the line element in Brinkmann coordinates as:

$$ds^2 = -2dudv + F(u, x, y)du^2 + dx^2 + dy^2 \quad (4)$$

where,  $u$  and  $v$  are null coordinates ( $u = \frac{1}{\sqrt{2}}(t + z)$ ,  $v = \frac{1}{\sqrt{2}}(t - z)$ ),  $x$  and  $y$  are the transverse spatial coordinates and the function  $F(u, x, y)$  encodes specific properties of the spacetime. Assuming the above line element as a solution of the vacuum Einstein equations one ends up requiring  $\partial_\alpha \partial^\alpha F = 0$  ( $\alpha$  being the spatial index representing  $x, y$ ). It is easily seen that

$$F(u, x, y) = W(u)(x^2 - y^2) \quad (5)$$

is a solution for  $\partial_\alpha \partial^\alpha F = 0$ , irrespective of the form of  $W(u)$ . It is this free function  $W(u)$  which we will choose to specify the gravitational wave pulse.

The string equations of motion in the pp-wave spacetime [10], for coordinates  $u, x, y$  are,

$$(\partial_\tau^2 - \partial_\sigma^2) u = 0 \quad (6)$$

$$(\partial_\tau^2 - \partial_\sigma^2) x = \frac{\partial_x F}{2} [(\partial_\tau u)^2 - (\partial_\sigma u)^2] \quad (7)$$

$$(\partial_\tau^2 - \partial_\sigma^2) y = \frac{\partial_y F}{2} [(\partial_\tau u)^2 - (\partial_\sigma u)^2] \quad (8)$$

and the equation for  $v$  is

$$\begin{aligned} (\partial_\tau^2 - \partial_\sigma^2) v = \frac{1}{2} (\partial_u F) [(\partial_\tau u)^2 - (\partial_\sigma u)^2] + (\partial_x F) [\partial_\tau u \partial_\tau x - \partial_\sigma u \partial_\sigma x] \\ + (\partial_y F) [\partial_\tau u \partial_\tau y - \partial_\sigma u \partial_\sigma y] \end{aligned} \quad (9)$$

Note that one can solve for the equations for  $u$ ,  $x$ ,  $y$  independently and then use the solutions in the R. H. S. of (9) to write the equation for  $v$ . The  $v$  equation can then be solved separately. A simple solution of the  $u$  equation is ( $p$ , a constant):

$$u = p\tau \quad (10)$$

This identifies the worldsheet time coordinate with the spacetime null coordinate  $u$ . With this choice, the two gauge conditions in Eqns (2) and (3) reduce to

$$p \partial_\sigma v = \partial_\tau x \partial_\sigma x + \partial_\tau y \partial_\sigma y \quad (11)$$

$$2p \partial_\tau v = p^2 F + (\partial_\tau x)^2 + (\partial_\sigma x)^2 + (\partial_\tau y)^2 + (\partial_\sigma y)^2 \quad (12)$$

It can easily be checked that the Eqns. (9), (10), (11) and (12) are mutually consistent and the following equations for  $x$  and  $y$  hold (using (10) in (7), (8)):

$$(\partial_\tau^2 - \partial_\sigma^2) x = \frac{p^2}{2} \partial_x F \quad (13)$$

$$(\partial_\tau^2 - \partial_\sigma^2) y = \frac{p^2}{2} \partial_y F \quad (14)$$

Therefore, given  $F$  one can find  $x$  and  $y$ , which can then be used in (11) and (12) to find  $v$ . We will now choose the  $W$  in  $F$  and try to solve for  $x$ ,  $y$  and  $v$ . Given  $F$  in the form in (5) and the assumption

$$x(\tau, \sigma) = (\cos k_1 \sigma) x(\tau) \quad (15)$$

$$y(\tau, \sigma) = (\sin k_1 \sigma) y(\tau) \quad (16)$$

we end up with the following equations for  $x(\tau)$  and  $y(\tau)$ .

$$\ddot{x} + (k_1^2 - p^2 W(\tau)) x = 0 \quad (17)$$

$$\ddot{y} + (k_1^2 + p^2 W(\tau)) y = 0 \quad (18)$$

where the dot denotes differentiation w.r.t.  $\tau$  (or, equivalently,  $u$  – except a constant factor ‘ $p$ ’). In the remote past when  $W(\tau)$  is zero we assume

$$x(\tau, \sigma) = R \cos k_1 \tau \cos k_1 \sigma \quad (19)$$

$$y(\tau, \sigma) = R \cos k_1 \tau \sin k_1 \sigma \quad (20)$$

which yields a circle with radius  $R \cos k_1 \tau$ , in the past. We will now assume different types of pulse profiles and solve the Eqns. (17) and (18). This will lead us to a ‘permanent change’ after the pulse has gone away—a feature known as the memory effect.

### III. CLOSED STRING EVOLUTION AND MEMORY

As mentioned above, we will solve Eqns. (17) and (18) with specific chosen inputs for  $W(\tau)$ , representing a pulse. Once the solutions for  $x(\tau)$  and  $y(\tau)$  subject to the initial conditions in (19), (20) are known, we will use them in (15), (16) to write down the profile functions  $x(\tau, \sigma)$  and  $y(\tau, \sigma)$ . Using the  $x(\tau, \sigma)$  and  $y(\tau, \sigma)$  in (11), (12) and integrating once we can obtain the profile  $v(\tau, \sigma)$ . Knowing all of  $u, v, x, y$  as functions of  $\tau$  and  $\sigma$  gives us the embedding of the string world sheet in the background  $pp$ -wave spacetime. Let us now proceed with the above scheme.

#### A. Square pulse

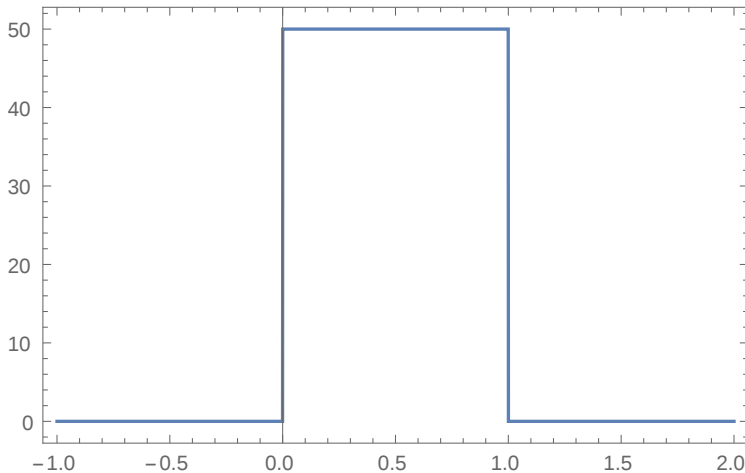


Figure. 2: The square pulse  $W$  as function of  $\tau$ .

To solve the equations for  $x(\tau)$  and  $y(\tau)$  we have to assume a functional form for  $W(\tau)$ . Here we choose it to be the following function (see Figure 2):

$$\begin{aligned}
 W(\tau) &= 0, & -\infty \leq \tau \leq 0 \\
 &= W_0, & 0 \leq \tau \leq T \\
 &= 0 & \tau \geq T
 \end{aligned}
 \tag{21}$$

This is the well-known square pulse. In order to solve the equations for  $x(\tau)$  and  $y(\tau)$  with the square pulse as  $W(\tau)$  we break up the domain of  $\tau$  into three regions ( $\tau \leq 0$ ,  $0 \leq \tau \leq T$  and  $\tau \geq T$ ), solve the equations in the three regions and thereafter match the functions and their derivatives at the two boundaries  $\tau = 0$  and  $\tau = T$ . In the region I ( $-\infty \leq \tau \leq 0$ ) we will assume  $x(\tau) = R \cos k_1 \tau$  and  $y(\tau) = R \cos k_1 \tau$ . Consequently, it turns out that  $x(\tau) = R \cos k_2 \tau$  and  $y(\tau) = R \cos k_3 \tau$  in region II (i.e. between  $0 \leq \tau \leq T$ ).

Finally, after some straightforward calculations, one arrives at the expressions for  $x(\tau)$  and  $y(\tau)$  in the  $\tau \geq T$  region. We have, for  $x(\tau, \sigma)$  and  $y(\tau, \sigma)$ :

$$x(\tau, \sigma) = R \left( \cos(k_2 T) \cos[k_1(\tau - T)] - \frac{k_2}{k_1} \sin(k_2 T) \sin[k_1(\tau - T)] \right) \cos(k_1 \sigma) \quad (22)$$

$$y(\tau, \sigma) = R \left( \cos(k_3 T) \cos[k_1(\tau - T)] - \frac{k_3}{k_1} \sin(k_3 T) \sin[k_1(\tau - T)] \right) \sin(k_1 \sigma) \quad (23)$$

where,

$$k_2 = \sqrt{k_1^2 - W_0 p^2} \quad ; \quad k_3 = \sqrt{k_1^2 + W_0 p^2} \quad (24)$$

It is easily evident from the expressions in (22) and (23) that the profile (in the  $xy$  plane) at any  $\tau \geq T$  is not a circle, even though it was a circle of radius ' $R \cos k_1 \tau$ ' before  $\tau = 0$ . For example, if we look at the profile at any value  $\tau = T + \frac{2n\pi}{k_1}$  ( $n = 0, 1, 2, \dots$ ) we always get

$$x = R \cos(k_2 T) \cos k_1 \sigma \quad ; \quad y = R \cos(k_3 T) \sin k_1 \sigma \quad (25)$$

Since  $k_2$  and  $k_3$  are never equal for  $W_0 \neq 0$ , the profile of the closed string in the  $xy$  plane, is an ellipse. One may track the shape of the closed string for different  $\tau \geq T$  and obtain the behaviour with the progress of  $\tau$ . It is easy to see that the ellipse changes its shape with the evolution of  $\tau$ . It does degenerate to a line along the  $x$  axis when the  $y$  coordinate becomes zero and vice versa. However, as is seen from the expression, it is never possible for both  $x$  and  $y$  to be zero or equal simultaneously. Therefore, we never see a circular string again. This is the 'permanent change' which is akin to a *memory effect caused by a gravitational wave pulse*. Figure 3 shows the string profile in the  $xy$  plane, at different increasing  $\tau \geq T$  values, in order to illustrate the permanent deformation of the closed circular string. Notice that the shape of the pulse plays a crucial role in creating this deformation, through the product  $W_0 T$  (height times the width).

It is possible to rewrite the above discussion in a general matrix notation. Let us consider column vectors  $\mathbf{X} = (x \ y)$ ,  $\mathbf{Q} = (\cos k_1 \sigma \ \sin k_1 \sigma)$  and write the above  $x, y$  profiles as a

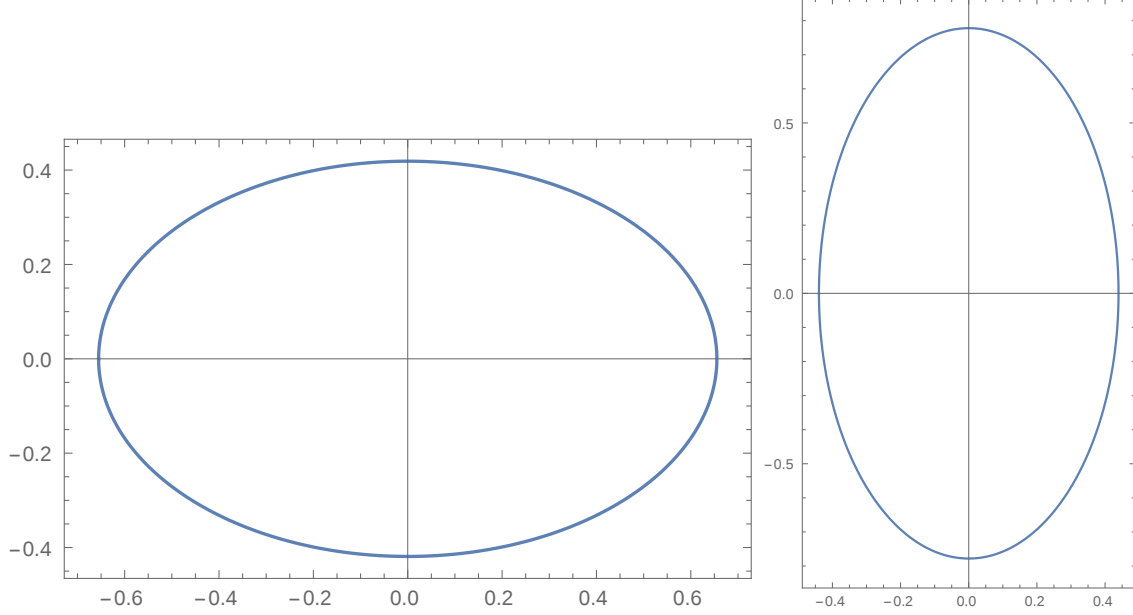


Figure. 3: The string profile in the  $xy$  plane for a square pulse, at two different values of  $u$  or  $\tau$ , after the pulse has left. The  $v$  coordinate is suppressed here. We have chosen  $T = 1$  unit,  $k_1T = 1$ ,  $k_2T = 0.5$ ,  $k_3T = \frac{\sqrt{7}}{2}$ ,  $R = 1$  unit. The  $\tau$  values are  $\tau = 1.5$  unit (left) and a later value,  $\tau = 1.8$  unit (right)

matrix equation,

$$\mathbf{X} = R \mathbf{A}^{-1} \mathbf{Q} \quad (26)$$

where  $\mathbf{A}^{-1}$  is the coefficient matrix. For the example discussed just above, this matrix has diagonal elements which can be read off from (22) and (23). In general, we obtain the relation,

$$\mathbf{X}^T (\mathbf{A}^T \mathbf{A}) \mathbf{X} = R^2 \quad (27)$$

The string will be a circle if

$$\mathbf{A}^T \mathbf{A} = h(\tau) \mathbf{I} \quad (28)$$

For  $\tau < 0$ , we get  $h(\tau) = (\cos k_1\tau)^{-2}$ . But, for  $\tau \geq T$ ,  $\mathbf{A}^T \mathbf{A}$  is not proportional to the identity matrix, which indicates the presence of a memory effect.

In order to complete this exercise, we must know the  $v$  coordinate too. This is a somewhat involved calculation and we may set  $p = \frac{k_1 R}{\sqrt{2}}$  ( as long as we choose to assume  $u = v$  before

the arrival of the pulse), to obtain an expression for  $v$  which will satisfy (11) and (12) with the inputs for  $x$  and  $y$  from (22) and (23). We end up with the following expressions in the three regions.

**Region  $\tau \leq 0$ :**

$$u = \frac{k_1 R}{\sqrt{2}} \tau \quad ; \quad v = \frac{k_1 R}{\sqrt{2}} \tau \quad (29)$$

$$x = R \cos k_1 \tau \cos k_1 \sigma \quad ; \quad y = R \cos k_1 \tau \sin k_1 \sigma \quad (30)$$

**Region  $0 \leq \tau \leq T$ :**

$$u = \frac{k_1 R}{\sqrt{2}} \tau \quad ; \quad x = R \cos k_2 \tau \cos k_1 \sigma \quad ; \quad y = R \cos k_3 \tau \sin k_1 \sigma \quad (31)$$

$$v(\tau, \sigma) = -\frac{R}{2\sqrt{2}} \frac{\cos 2k_1 \sigma}{k_1^2} G_0(\tau) + H_0(\tau) \quad (32)$$

where,

$$G_0(\tau) = k_1 k_2 \cos k_2 \tau \sin k_2 \tau - k_1 k_3 \cos k_3 \tau \sin k_3 \tau$$

and

$$H_0(\tau) = \frac{k_1 R}{\sqrt{2}} \tau + \frac{k_1^2 - k_2^2}{2\sqrt{2}k_1} R \left( \frac{\sin(2k_2 \tau)}{2k_2} - \frac{\sin(2k_3 \tau)}{2k_3} \right) \quad (33)$$

**Region  $\tau \geq T$ :**

$$u = \frac{k_1 R}{\sqrt{2}} \tau \quad ; \quad v(\tau, \sigma) = -\frac{R}{2\sqrt{2}} \frac{\cos 2k_1 \sigma}{k_1^2} G(\tau) + H(\tau) \quad (34)$$

where,

$$\begin{aligned} G(\tau) = & \frac{1}{2} (k_1^2 \cos^2 k_2 T - k_2^2 \sin^2 k_2 T) \sin 2k_1(\tau - T) + k_1 k_2 \cos k_2 T \sin k_2 T \cos 2k_1(\tau - T) \\ & - \frac{1}{2} (k_1^2 \cos^2 k_3 T - k_3^2 \sin^2 k_3 T) \sin 2k_1(\tau - T) - k_1 k_3 \cos k_3 T \sin k_3 T \cos 2k_1(\tau - T) \end{aligned} \quad (35)$$

and

$$\begin{aligned} H(\tau) = & \frac{R}{2\sqrt{2}k_1} (k_1^2 \cos^2 k_2 T + k_2^2 \sin^2 k_2 T + k_1^2 \cos^2 k_3 T + k_3^2 \sin^2 k_3 T) (\tau - T) + \\ & \frac{k_1 R}{\sqrt{2}} T + \frac{k_1^2 - k_2^2}{2\sqrt{2}k_1} R \left( \frac{\sin(2k_2 T)}{2k_2} - \frac{\sin(2k_3 T)}{2k_3} \right) \end{aligned} \quad (36)$$

with  $x$  and  $y$  for  $\tau \geq T$  as given in (22), (23).

It can be verified that the above forms of  $x$ ,  $y$ ,  $u$  and  $v$  match at the boundaries  $\tau = 0$  and  $\tau = T$ . The  $v$  coordinate exhibits a derivative discontinuity at the boundaries because of the piece-wise continuous nature of the square pulse.

The above analysis shows that before the pulse arrives, the centre of mass of the string (given via  $z = \frac{1}{\sqrt{2}}(u - v)$ ) is at  $z = 0$ . However, after the pulse arrives and leaves, the centre of mass develops a translational motion in  $\tau$  as well as an oscillation. One can go over to a Lorentz frame (Lorentz transformation in the  $t, z$  coordinates) and make sure that the centre of mass has only oscillatory motion after the pulse leaves. With such a Lorentz transformation the new  $u, v$  coordinates (named as  $u', v'$ ) become:

$$u' = \sqrt{a} \frac{k_1 R}{\sqrt{2}} \tau \quad (37)$$

$$v' = \sqrt{a} \frac{k_1 R}{\sqrt{2}} \tau + \frac{k_1 R b}{\sqrt{2a}} - \frac{R}{2\sqrt{2a}} \frac{\cos 2k_1 \sigma}{k_1^2} G(\tau) \quad (38)$$

where  $a$  and  $b$  are, as defined in  $H(\tau) = \frac{k_1 R}{\sqrt{2}} (a\tau + b)$  with

$$a = \frac{1}{2k_1^2} (k_1^2 \cos^2 k_2 T + k_2^2 \sin^2 k_2 T + k_1^2 \cos^2 k_3 T + k_3^2 \sin^2 k_3 T) \quad (39)$$

$$b = -\frac{1}{2k_1^2} (k_1^2 \cos^2 k_2 T + k_2^2 \sin^2 k_2 T + k_1^2 \cos^2 k_3 T + k_3^2 \sin^2 k_3 T) T + T + \frac{k_1^2 - k_2^2}{2k_1^2} \left( \frac{\sin(2k_2 T)}{2k_2} - \frac{\sin(2k_3 T)}{2k_3} \right) \quad (40)$$

and the magnitude of the boost velocity between the two frames is given as  $v_{boost} = \frac{1-a}{1+a}$ . For  $a > 1$ ,  $v_{boost} \rightarrow -v_{boost}$  and one needs to replace  $a$  with  $\frac{1}{a}$  in the above formulae. Further, from  $u'$  and  $v'$  one can obtain  $t'$  and  $z'$ .

The emerging picture of the closed string before and after it experiences the pulse is as follows:

- Before the pulse arrives the closed string shape is circular and its centre of mass is at  $z = 0$ . The radius of the circle changes with  $\tau$  (a pulsating string) and can even become zero at specific  $\tau$  values. The  $v$  coordinate is chosen to have the same value as the  $u$  coordinate, for any  $\tau$ . In fact  $u = v$  as in Eqn. (29).
- After the pulse departs, the closed string profile in the  $xy$  plane (at a fixed  $\tau$  value) is elliptical in shape and never becomes circular. If we include the behaviour of the  $v$  coordinate, we can see from (32) or (34) that for fixed  $\tau$ ,  $v$  has different values at different  $\sigma$ . In fact, at fixed  $\tau$ , one can relate the spacetime coordinate  $v$  with the worldsheet coordinate

$\sigma$ , for the given embedding. The shape of the string can degenerate to a line (along  $x$  or  $y$ ) at specific  $\tau$  values. The centre of mass ( $z' = \frac{1}{\sqrt{2}}(u' - v')$  value) is now purely oscillatory with different amplitudes at different  $\tau$  (construct  $z'$  from (37), (38)) – it does not have any linear in  $\tau$  motion as long as we are in a properly chosen frame. Note that prior to the arrival of the pulse, the centre of mass was at  $z = 0$  (see Eqn. (29)). The string profiles in  $xyz'$  space at chosen values of  $\tau$  are shown in Figure 4. One can see that before the pulse arrives, the string is confined to the  $z = 0$  plane, though later, it spreads out.

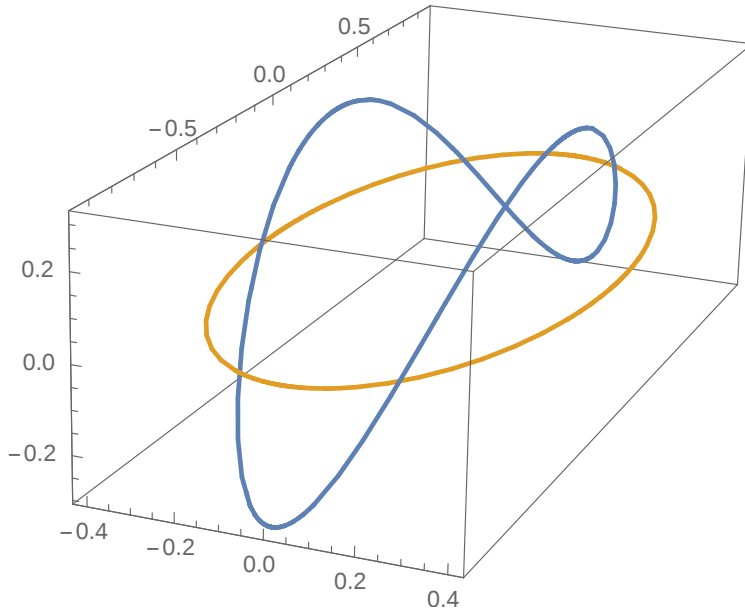


Figure. 4: The string profile in  $xyz'$  space for a square pulse, at two different values of  $u$  or  $\tau$ , before the arrival (yellow curve) and after the departure (blue curve) of the pulse. We have chosen  $T = 1$  unit,  $k_1T = 1$ ,  $k_2T = 0.5$ ,  $k_3T = \frac{\sqrt{7}}{2}$ ,  $R = 1$  unit. Eqns (22), (23) and (37)-(40) are used. The  $\tau$  values are  $\tau = -2$  unit (yellow) and a later value,  $\tau = 2$  unit (blue). The vertical axis is the  $z'$  axis.

There are changes in the geometry of the worldsheet caused by the pulse. We will discuss these aspects briefly in the penultimate section of this article.

### B. Sech-squared pulse

It is easy to redo the above analysis for a delta function pulse ( $W(\tau) = W_0\delta(\tau)$ ). The results are similar to the square pulse and the mathematical details have been worked out

in [10], though the authors in [10] unfortunately missed mentioning the ‘memory’ aspect! The square and the delta function pulses are largely idealistic. We therefore move on now to a pulse shape which is smooth—the so-called sech-squared pulse. The  $W(\tau)$  here is given as (see Figure 5):

$$W(\tau) = \frac{\alpha^2}{4p^2} \operatorname{sech}^2 \alpha \tau \quad (41)$$

The two differential equations which we need to solve to obtain  $x(\tau)$  and  $y(\tau)$  are,

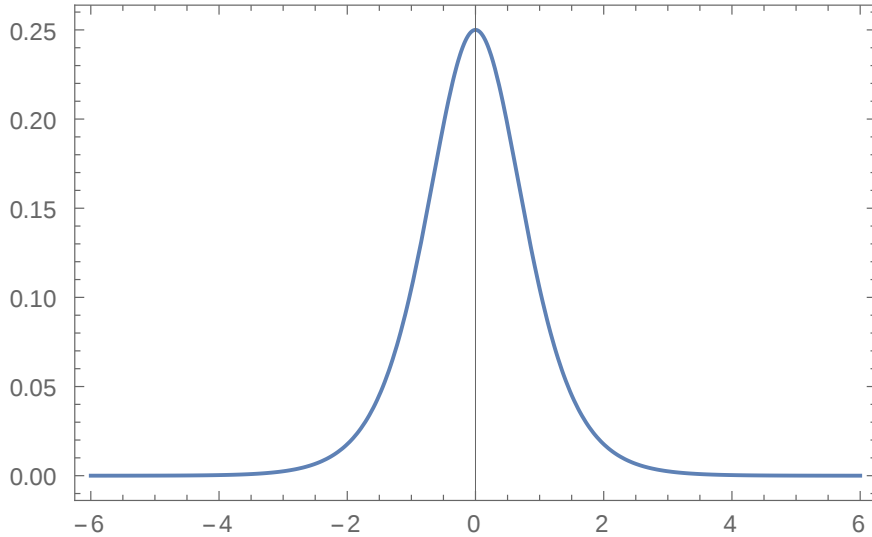


Figure. 5: The Sech-squared pulse  $W$  as function of  $\tau$  (or  $u$ ). Here  $\alpha = 1$ .

$$\ddot{x} + \left( k_1^2 - \frac{\alpha^2}{4} \operatorname{sech}^2 \alpha \tau \right) x = 0 \quad (42)$$

$$\ddot{y} + \left( k_1^2 + \frac{\alpha^2}{4} \operatorname{sech}^2 \alpha \tau \right) y = 0 \quad (43)$$

Both these equations can be solved exactly and the asymptotic forms of the solutions are known. As we did earlier, we will impose the circular closed string shape at negative infinity (i.e.  $\tau \rightarrow -\infty$ ). Using the known asymptotic forms we will then find out the shape of the closed string as  $\tau \rightarrow \infty$ . A change in the shape, like before, will be associated with a permanent deformation and a memory effect caused by the pulse.

The Eqns. (42) and (43) fall in the general class of Pöschl–Teller potential problems usually studied in quantum mechanics [49]. The two linearly independent solutions for equations of the type

$$\ddot{U}(\tau) + \left( k^2 + \frac{\alpha^2 \lambda(\lambda - 1)}{\cosh^2 \alpha \tau} \right) U(\tau) = 0 \quad (44)$$

are given as

$$\begin{aligned} U_1(\tau) &= (1 + \tanh \alpha\tau)^{\frac{ik}{2\alpha}} (1 - \tanh \alpha\tau)^{-\frac{ik}{2\alpha}} {}_2F_1 \left( \lambda; 1 - \lambda; \frac{ik}{\alpha} + 1; \frac{1 + \tanh \alpha\tau}{2} \right) \\ U_2(\tau) &= 2^{\frac{ik}{\alpha}} (1 - \tanh^2 \alpha\tau)^{-\frac{ik}{2\alpha}} {}_2F_1 \left( \lambda - \frac{ik}{\alpha}; 1 - \lambda - \frac{ik}{\alpha}; 1 - \frac{ik}{\alpha}; \frac{1 + \tanh \alpha\tau}{2} \right) \end{aligned} \quad (45)$$

where  ${}_2F_1$  denotes the hypergeometric function. The general solution therefore is,

$$U(\tau) = AU_1(\tau) + BU_2(\tau) \quad (46)$$

where  $A$  and  $B$  are constants to be determined by the initial conditions. Eqn. (44) will match with (42) when  $\lambda = \frac{1}{2}$ . Similarly, when  $\lambda = \frac{1+\sqrt{2}}{2}$  we will get Eqn. (43).

We now need to write down the asymptotic form of the general solution in (45) for  $\tau \rightarrow -\infty$  and  $\tau \rightarrow +\infty$ .

Notice that for  $\tau \rightarrow -\infty$ , the argument of the hypergeometric function goes to zero and the value of  ${}_2F_1(a; b; c; 0)$  is equal to one. Hence, expanding the hyperbolic tangents as exponentials and taking the limit  $\tau \rightarrow -\infty$  we have

$$U(\tau \rightarrow -\infty) = Ae^{ik\tau} + Be^{-ik\tau} \quad (47)$$

The limit of  $\tau \rightarrow +\infty$  is a little tricky to obtain. One will have to use a linear transformation formula [50], [?] and write the hypergeometric function with the argument  $z = \frac{1+\tanh \alpha\tau}{2}$  in terms of a sum (with a  $z$  dependent coefficient) of two hypergeometric functions with arguments  $1 - z = \frac{1-\tanh \alpha\tau}{2}$ . This helps in getting the asymptotic form easily because, now, as one takes the limit  $\tau \rightarrow \infty$  one ends up with the argument as zero in the two hypergeometric functions and their value become equal to one.

Thus, as  $\tau \rightarrow \infty$  one gets

$$U(\tau \rightarrow \infty) = A'e^{ik\tau} + B'e^{-ik\tau} \quad (48)$$

where

$$A' = \frac{\Gamma(\frac{ik}{\alpha} + 1)\Gamma(\frac{ik}{\alpha})}{\Gamma(\frac{ik}{\alpha} + 1 - \lambda)\Gamma(\frac{ik}{\alpha} + \lambda)} A + \frac{\Gamma(1 - \frac{ik}{\alpha})\Gamma(\frac{ik}{\alpha})}{\Gamma(1 - \lambda)\Gamma(\lambda)} B = a_1 A + b_1 B \quad (49)$$

$$B' = \frac{\Gamma(\frac{ik}{\alpha} + 1)\Gamma(-\frac{ik}{\alpha})}{\Gamma(1 - \lambda)\Gamma(\lambda)} A + \frac{\Gamma(1 - \frac{ik}{\alpha})\Gamma(-\frac{ik}{\alpha})}{\Gamma(\lambda - \frac{ik}{\alpha})\Gamma(1 - \lambda - \frac{ik}{\alpha})} B = a_2 A + b_2 B \quad (50)$$

Armed with these asymptotic forms we will now write down the solutions for Eqns. (42) and (43).

Let us first consider Eqn. (42), i.e. the  $x$  equation. We keep in mind that we need to use  $\lambda = \frac{1}{2}$  while using the solutions quoted above. Here, as  $\tau \rightarrow -\infty$  we need  $x(\tau) = R \cos k_1 \tau$  (and  $x(\tau, \sigma) = R \cos k_1 \tau \cos k_1 \sigma$ ). Therefore, one has to choose  $A = B = \frac{R}{2}$ . With this asymptotic condition at  $\tau \rightarrow -\infty$ , one can easily write down the final solution for  $\tau \rightarrow \infty$ . This is given as (taking the real part of the full complex solution, since  $a_1, b_1, a_2, b_2$  can be complex):

$$x(\tau, \sigma) = \frac{R}{2} \text{Re} [(a_1 + b_1 + a_2 + b_2) \cos k_1 \tau \cos k_1 \sigma + (a_2 + b_2 - a_1 - b_1) \sin k_1 \tau \sin k_1 \sigma + i(a_1 + b_1 - a_2 - b_2) \sin k_1 \tau \cos k_1 \sigma + i(a_1 + b_1 + a_2 + b_2) \cos k_1 \tau \sin k_1 \sigma] \quad (51)$$

For Eqn. (43), we need to use  $\lambda = \frac{1+\sqrt{2}}{2}$ . The  $\tau \rightarrow -\infty$  asymptotic form of  $y(\tau, \sigma)$  is given as  $R \cos k_1 \tau \sin k_1 \sigma$ . To implement this form in the asymptotic past, we will need to use  $A = B = \frac{R}{2i}$  in the solutions quoted above. We will write the final results using  $a'_1, b'_1, a'_2$  and  $b'_2$  since we have a different equation and a different  $\lambda$  value. Thus, we have  $y(\tau, \sigma)$  as:

$$y(\tau, \sigma) = \frac{R}{2} \text{Re} [-i(a'_1 + b'_1 + a'_2 + b'_2) \cos k_1 \tau \cos k_1 \sigma - i(a'_2 + b'_2 - a'_1 - b'_1) \sin k_1 \tau \sin k_1 \sigma + (a'_1 + b'_1 - a'_2 - b'_2) \sin k_1 \tau \cos k_1 \sigma + (a'_1 + b'_1 + a'_2 + b'_2) \cos k_1 \tau \sin k_1 \sigma] \quad (52)$$

It is evident from the above expressions that the circular string in the asymptotic past, under the influence of the gravitational wave pulse will change its shape and become elliptical in shape, in the asymptotic future. To see this explicitly, we will now work out the details with explicit values for the various parameters and then plot the profiles. We have chosen to retain values upto four decimal places.

Let us consider the case where  $k_1 = 1, \alpha = 1$ . Using the expressions  $a_1, a_2, b_1, b_2$  with  $\lambda = \frac{1}{2}$  we obtain

$$x(\tau, \sigma) = \frac{R}{2} (1.9379 \cos \tau + 0.6971 \sin \tau) \cos \sigma \quad (53)$$

For  $\lambda = \frac{1+\sqrt{2}}{2}$  and the same  $k_1, \alpha$  one gets, using  $a'_1, b'_1, a'_2$  and  $b'_2$ ,

$$y(\tau, \sigma) = \frac{R}{2} (1.9461 \cos \tau - 0.5777 \sin \tau) \sin \sigma \quad (54)$$

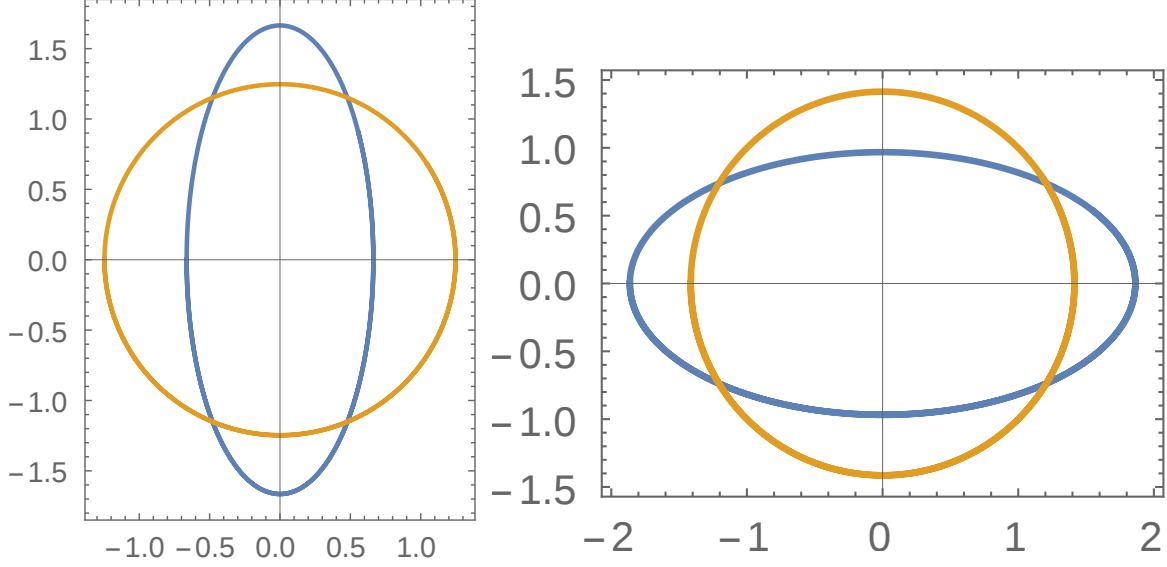


Figure. 6: The late time string configurations (blue curves) at  $\tau = \frac{103\pi}{7}$  (left) and at  $\tau = \frac{101\pi}{4}$  (right). The yellow circles correspond to the earlier configurations at  $\tau = -\frac{103\pi}{7}$  and  $\tau = -\frac{101\pi}{4}$ . We have assumed  $R = 2$  units and Eqns. (19), (20) and (53), (54).

The expressions are, by definition, the profiles at large values of  $\tau$ . However, we can get an idea of the elliptical shape by plotting at a large, finite value of  $\tau$ . Two representative plots are shown in Figure 6. The initial profile (at  $\tau \rightarrow -\infty$ ) is just a circle ( $x = 2 \cos \tau \cos \sigma$ ,  $y = 2 \cos \tau \sin \sigma$ ).

A permanent change in the shape of the string appears to have taken place. The cause of this is, like in the square pulse case, the gravitational wave pulse – given here as a sech-squared function of  $\tau$  or  $u$ .

It is possible to obtain  $v(\tau, \sigma)$  in this case too though we do not attempt to analyse it here. Qualitatively, the result is not expected to be very different from the square pulse case discussed earlier.

#### IV. WORLDSHEET GEOMETRY AND MEMORY

Let us now focus on the geometry of the worldsheet. We will consider here the case of the square pulse only. The worldsheet line element can be found using the embedding functions and the worldsheet metric functions  $\gamma_{ab} = g_{ij} \partial_a x^i \partial_b x^j$ . As expected, the line element is

diagonal (conformal gauge choice). We have, for  $\tau \leq 0$ , the line element as given by,

$$ds_{\tau \leq 0}^2 = R^2 k_1^2 \cos^2 k_1 \tau (-d\tau^2 + d\sigma^2) \quad (55)$$

The metric is degenerate (zero determinant) at all  $\tau = \frac{(2n+1)\pi}{2k_1}$  ( $n = 0, 1, 2, \dots$ ).

On the other hand the line element for  $\tau \geq T$  is given as

$$ds^2 = \Omega^2(\tau, \sigma) (-d\tau^2 + d\sigma^2) \quad (56)$$

where

$$\begin{aligned} \Omega^2(\tau, \sigma) = R^2 \sin^2 k_1 \sigma [k_1 \cos k_2 T \cos k_1(\tau - T) - k_2 \sin k_2 T \sin k_1(\tau - T)]^2 + \\ R^2 \cos^2 k_1 \sigma [k_1 \cos k_3 T \cos k_1(\tau - T) - k_3 \sin k_3 T \sin k_1(\tau - T)]^2 \end{aligned} \quad (57)$$

The metric here is never degenerate if  $\Omega^2(\tau, \sigma)$  is not zero for any value of  $\tau, \sigma$ . How do we check this? Since  $\Omega^2$  is a sum of two squares, it can only be zero if the individual terms are both zero. This seems possible, say at  $\tau = \tau_c$ , if  $k_2 \tan k_2 T = k_3 \tan k_3 T = \frac{k_1}{\nu}$ , where  $\tan k_1(\tau_c - T) = \nu$ . Further, we have  $k_2 < k_3$  and  $k_2^2 + k_3^2 = 2k_1^2$ . It is possible to solve the first equation, i.e.  $k_2 \tan k_2 T = k_3 \tan k_3 T$ , to arrive at a value of  $T$  (given  $k_1, k_2$ ). This value of  $T$  can then be used in the other equation, i.e.  $k_2 \tan k_2 T = k_1 \cot k_1(\tau_c - T)$ , to obtain  $\tau_c$ . For example, assuming, in appropriate units,  $k_1 = \frac{5}{\sqrt{2}}$ ,  $k_2 = 3$  and  $k_3 = 4$ , we can easily see that  $T = m\pi$  solves the first equation. Using  $m = 1$ , we get one value  $\tau_c = \pi(1 + \frac{\sqrt{2}}{10})$  (others are there too) from the second equation. In fact,  $T = m\pi$  will always satisfy the first equation as long as  $k_2, k_3$  are integers satisfying the previously stated constraints. Hence, at such  $\tau$  values, for the specific  $T$ , one does get  $\Omega^2 = 0$ , but, for all other  $T$  one can have  $\Omega^2 \neq 0$  everywhere. Therefore, if the pulse is such that its width  $T$  is different from the set of  $T$  values which yield  $\Omega^2 = 0$  at some  $\tau = \tau_c$ , one does indeed end up with a non-degenerate metric.

The Ricci scalar  $\mathcal{R}$  of the two dimensional worldsheet also undergoes a change in character after the passage of the pulse. Recall that the expression for the Ricci scalar in terms of the conformal factor  $\Omega^2$  is

$$\mathcal{R} = -\frac{2}{\Omega^2} \left( -\frac{\partial^2}{\partial \tau^2} + \frac{\partial^2}{\partial \sigma^2} \right) \ln \Omega \quad (58)$$

The denominator factor in the above expression can lead to a worldsheet singularity where  $\Omega^2 = 0$ . Thus, singularities always exist prior to the arrival of the pulse, but may get removed (depending on the value of  $T$  for the pulse) after its passage.

Both the above features— (a) metric becoming non-degenerate everywhere and (b) the worldsheet singularities being removed — are ‘permanent changes’ which could possibly be caused by the gravitational wave pulse. Thus, apart from the change of shape of the circular string, we may also see changes in the worldsheet geometry which seem to add on to the character of ‘memory’.

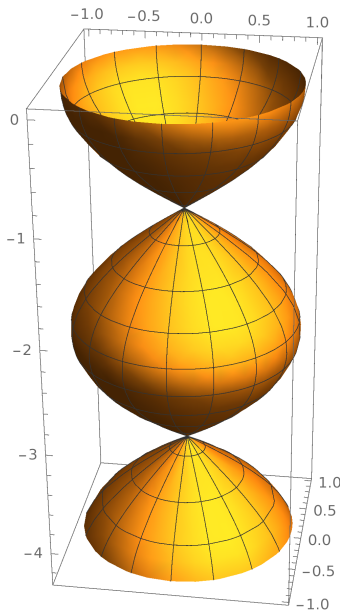


Figure. 7: The worldsheet geometry before the arrival of the pulse. The zero radius locations are the worldsheet singularities. We have used Eqns. (29), (30) with  $R = 1$ .  $k_1\tau$  and  $k_1\sigma$  are the surface coordinates.

One can visualise the two dimensional surface of the worldsheet by embedding it in a three dimensional Euclidean background. The string worldsheet however is a two dimensional surface in the four dimensional pp-wave spacetime, which, as we noted before, is just flat spacetime before and after the duration of the pulse. Embeddings as hypersurfaces in Euclidean space can therefore provide only a partial visualisation. We show the embedded (in a three dimensional background) sections of the worldsheet geometry in Figures 7-9.

Figure 7 shows the embedding  $(x(\tau, \sigma), y(\tau, \sigma), u(\tau) = \frac{1}{\sqrt{2}}\tau)$  before the arrival of the pulse. One can see the presence of singularities on the worldsheet at locations where it collapses to a point. As mentioned before, it is a pulsating string. Here, i.e. prior to the arrival of the pulse, the embedding  $(x(\tau, \sigma), y(\tau, \sigma), v(\tau) = \frac{1}{\sqrt{2}}\tau)$  is the same as the  $xyu$  embedding.

Figure 8 shows the worldsheet after the pulse departs. One can see here that the worldsheet

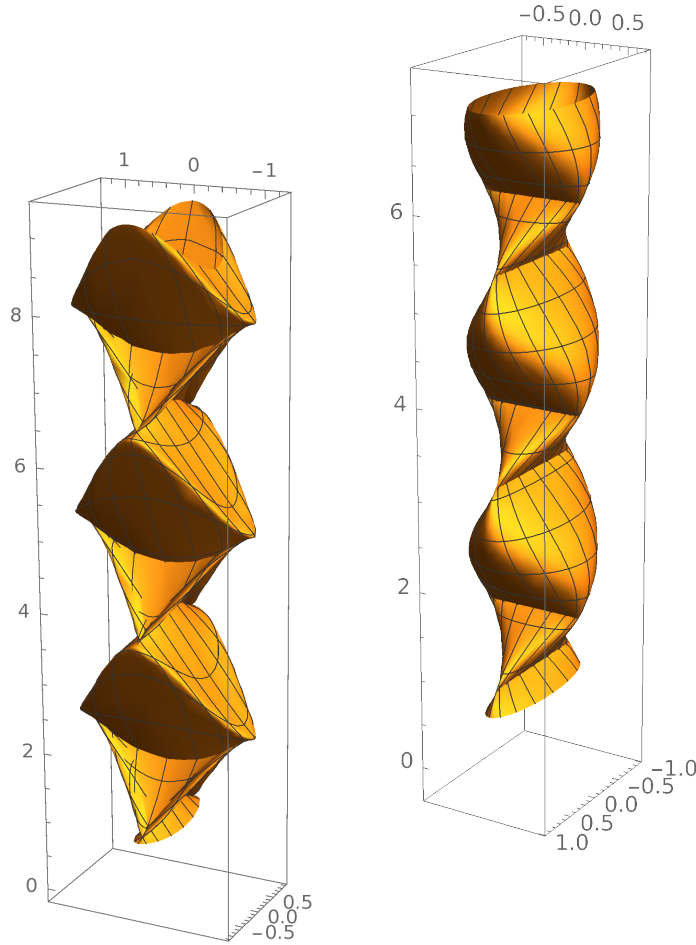


Figure. 8: The worldsheet geometry as a  $xyv$  embedding (left) and a  $xyu$  embedding (right) after the departure of the pulse. There are no locations where the worldsheet shrinks to a point. Hence, no worldsheet singularities. Eqns. (22), (23) and (34)-(36) are used with values for the parameters  $T$ ,  $k_1T$ ,  $k_2T$ ,  $k_3T$  and  $R$  as mentioned for Figure 3.

The surface coordinates are  $k_1\tau$  and  $k_1\sigma$ .

is indeed nonsingular – it never collapses to a point—at best it can collapse to a line. The plot (left) is obtained by using the parametric relations for  $x(\tau, \sigma)$ ,  $y(\tau, \sigma)$  and  $v(\tau, \sigma)$ . Since  $u$  is proportional to  $\tau$ , the spacetime null coordinate  $u$  is proportional to the worldsheet ‘time’  $\tau$ . Before the pulse arrives  $u = v$ , but later it is not so. The embedding  $x(\tau, \sigma)$ ,  $y(\tau, \sigma)$  and  $u(\tau)$  is shown on the right, in Figure 8, where the nonsingular nature of the worldsheet is perhaps more clearly visible. For the embedding  $xyv$ , at any  $\tau$  value, points at different  $\sigma$  do not lie on a plane and the string is spread away from any  $u = \text{constant}$  plane. This does

not happen for the  $xyu$  embedding. Further, one can construct  $xyz'$  and  $xyt'$  embeddings which are shown in Figure 9. One may note the connection between the blue curve (at one later  $\tau$  value) in Figure 4 and the finite zone (over the range for  $\tau$ ) within which the string wraps itself while evolving (as displayed in the  $xyz'$  embedding), in Figure 9.

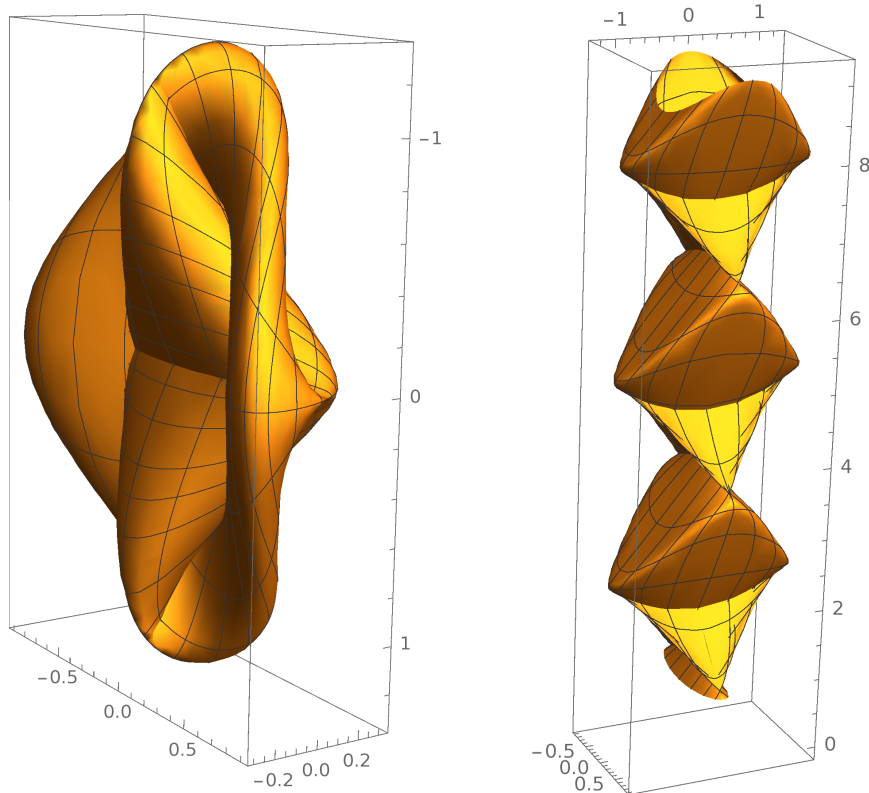


Figure. 9: The worldsheet geometry as a  $xyz'$  embedding (left) and a  $xyt'$  embedding (right), after the arrival of the pulse. Eqns. (22), (23) and expressions for  $t'$  and  $z'$  (derived from Eqns. (37) - (40)) are used with values for the parameters  $T$ ,  $k_1T$ ,  $k_2T$ ,  $k_3T$  and  $R$ , as mentioned in Figure 3. The surface coordinates are  $k_1\tau$  and  $k_1\sigma$ .

All the above ‘visualisations’ are of some use in our attempt to understand the nature of the worldsheet in the four dimensional spacetime. As stated earlier, since the string worldsheet is a codimension two surface in a four dimensional background one needs to look at different embeddings in order to develop a clear picture. Since, in a pp-wave spacetime, the coordinate  $u$  is a parameter that can label points on a geodesic curve (observer) and  $u$  is identified (except for a constant  $p$ ) with the worldsheet coordinate  $\tau$ , the change of shape from a circle to an ellipse in the  $xy$  plane (before and after the pulse) is seen only in the  $xyu$  embedding. In the other embeddings, the string is a closed space curve (not circular),

as is visible in Figure 4.

## V. CONCLUSIONS

Our main objective in this article was to show how a gravitational wave pulse can affect the shape of string as it evolves to generate the worldsheet. As mentioned in the Introduction, our motivation was to provide a ‘stringy’ realisation of the often used picture where memory is linked to the ‘permanent change’ in the shape of a ring of particles. We achieve this goal by studying strings in pp-wave spacetimes where the gravitational wave pulse is modeled by the free function available in such spacetimes. Studying strings in the presence of a square and a sech-squared pulse we show that a circular string in the past (before the arrival of the pulse) evolves into a deformed shape (ellipse, in the  $xy$  plane) in the asymptotic future. The satisfying fact is that we are able to demonstrate this explicitly by solving all relevant equations analytically.

It may be argued that the shape of the string is a coordinate dependent feature and one should look for quantities which do not depend on the choice of background coordinates. We have shown, towards the end of our article, that there exist such quantities which may exhibit a permanent change – the behaviour of the metric determinant and the Ricci scalar of the worldsheet metric being two such quantities. Both of them could possibly exhibit a ‘permanent change’, the details of which have been demonstrated clearly in the previous section. In addition, the different embeddings of the worldsheet in a three dimensional Euclidean background provide a useful way of visualising the changes that occur after the duration of the pulse. One may also consider finding the energy (target space) of the string using the expression  $P^0 = -T_0 \int_0^{2\pi} \sqrt{-\gamma} \gamma^{\tau a} (\partial_a x^0) d\sigma$ . Working through this calculation (not quoted here) we did find a difference between the expressions for ‘before’ and ‘after’ the pulse, which is also a signature of memory.

It is possible to work on this topic further and find more examples. We have indeed found very similar effects for a triangular pulse as well as a completely general pulse shape replacing the non-zero constant in the square case. In all scenarios though we do find a ‘permanent change’. One is tempted to ask therefore—what kind of pulse will show no change in shape of a string? Another open question is related to the use of a more general Kundt wave spacetime background. One can investigate strings in such Kundt spacetimes and look for

a similar memory effect [35], [36] and its consequences.

## ACKNOWLEDGEMENTS

AD thanks the Department of Physics, IIT Kharagpur, India for the opportunity to do a part of this work during his fourth year bachelors project in 2023-24.

- 
- [1] M. Favata, *Class. Quant. Grav.* **27**, 084036 (2010).
  - [2] M. Favata, [Lecture slides](#).
  - [3] B. Zwiebach, *A first course in string theory*, Cambridge University Press, Cambridge, UK (2004).
  - [4] J. B. Griffiths and J. Podolsky, *Exact Space-Times in Einstein's General Relativity*, Cambridge University Press, Cambridge, UK (2009).
  - [5] M. Blau, *Lectures on 'Plane waves and Penrose limits'* [Lecture notes](#).
  - [6] D. Amati and C. Klimcik, *Phys. Letts.* **B210**, 92 (1988).
  - [7] G. T. Horowitz and A. Steif, *Phys. Rev.* **D 42**, 1950 (1990).
  - [8] H. J. de Vega and N. Sanchez, *Phys. Rev.* **D45**, 2783 (1992).
  - [9] H. J. de Vega, M. Ramon-Medrano and N. Sanchez, *Class. Quant. Grav.* **10**, 2007 (1993).
  - [10] V. Liška and R. von Unge, *Phys. Rev.* **D106**, 044066 (2022).
  - [11] H. Afshar, E. Esmacili and M. M. Sheikh-Jabbari, *JHEP02*, 053 (2019).
  - [12] A. Aldi, M. Bianchi and M. Firrotta, *Phys. Letts.* **B 813**,136037 (2021).
  - [13] O. M. Boersma, D. A. Nichols, P. Schmidt, *Phys. Rev.* **D 101**, 083026 (2020).
  - [14] M. Hübner, P. Lasky, E. Thrane, *Phys. Rev.* **D 104**, 023004 (2021).
  - [15] A. Grant and D. A. Nichols, *Phys.Rev.* **D 107**, 064056 (2023).
  - [16] S. Y. Cheung, P. D. Lasky and E. Thrane, *Class. Quant. Grav.* **41**, 115010 (2024).
  - [17] H. Inchauspé, S. Gasparotto, D. Blas, L. Heisenberg, J. Zosso, S. Tiwari, [arXiv:2406.09228](#).
  - [18] Y. B. Zel'dovich and A. G. Polnarev, *Sov. Astron* **18**, 17 (1974).
  - [19] V. B. Braginsky and L. P. Grishchuk, *Sov. Phys. JETP* **62**, 427 (1985).
  - [20] D. Christodoulou, *Phys. Rev. Lett.* **67**, 1486 (1991).
  - [21] L. Bieri and D. Garfinkle, *Phys. Rev.* **D 89**, 084039 (2014).

- [22] A. Tolish, L. Bieri, D. Garfinkle, and R. M. Wald, Phys. Rev. **D 90**, 044060 (2014).
- [23] A. Tolish and R. M. Wald, Phys. Rev. **D 89**, 064008 (2014).
- [24] T. Mädler and J. Winicour, Class. Quant. Grav. **33**, 175006 (2016).
- [25] T. Mädler and J. Winicour, Class. Quant. Grav. **34**, 115009 (2017).
- [26] A. Strominger and A. Zhiboedov, J. High Energy Phys. **01** (2016), 86.
- [27] A. Strominger, Lectures on the Infrared Structure of Gravity and Gauge Theory (2017) [arXiv:1703.05448](https://arxiv.org/abs/1703.05448) [hep-th].
- [28] P.-M. Zhang, C. Duval, G. W. Gibbons, and P. A. Horvathy, Phys. Lett. **B 772**, 743 (2017).
- [29] P.-M. Zhang, C. Duval, G. W. Gibbons, and P. A. Horvathy, Phys. Rev. **D 96**, 064013 (2017).
- [30] P. M. Zhang, C. Duval, G. W. Gibbons, and P. A. Horvathy, JCAP **05**, 030.
- [31] P.-M. Zhang, C. Duval, and P. A. Horvathy, Class. Qtm. Grav. **35**, 065011 (2018).
- [32] P. M. Zhang, M. Elbistan, G. W. Gibbons, and P. A. Horvathy, Gen. Rel. Grav. **50**,107 (2018).
- [33] I. Chakraborty and S. Kar, Phys. Rev. **D 101**, 064022 (2020).
- [34] B. Cvetković and D. Simić, Eur. Phys. J. C **82**, 127 (2022).
- [35] I. Chakraborty and S. Kar, Phys. Lett. **B 808**, 135611 (2020).
- [36] S. Siddhant, I. Chakraborty, and S. Kar, Eur. Phys. J. C **81**, 350 (2021).
- [37] I. Chakraborty and S. Kar, Eur. Phys. J. Plus **137**, 418 (2022).
- [38] J. Ben Achour and J-P Uzan, [arXiv:2406.07106](https://arxiv.org/abs/2406.07106).
- [39] P. -M. Zhang and P. A. Horvathy, [arXiv:2405.12928](https://arxiv.org/abs/2405.12928).
- [40] E. E. Flanagan, A. M. Grant, A. I. Harte and D. A. Nichols, Phys. Rev. **D 99**, 084004 (2019).
- [41] E. E. Flanagan, A. M. Grant, A. I. Harte and D. A. Nichols, Phys. Rev. D **101**, 104033 (2020).
- [42] A. M. Grant and D. A. Nichols, Phys. Rev. **D 105**, 024056 (2022).
- [43] A. Grant, Class. Quant. Grav. **41**, 175004 (2024).
- [44] M. O’Loughlin and H. Demirchian, Phys. Rev. **D 99**, 024031 (2019).
- [45] A. K. Divakarla and B. F. Whiting, Phys. Rev. D **104**, 064001 (2021).
- [46] G. M. Shore, JHEP **12**, 133 (2018).
- [47] H. Hadi, A. R. Akbarieh, David F. Mota, Class. Quantum Grav. **41**, 105005 (2024).
- [48] K. Mitman, M. Boyle, L. C. Stein, N. Deppe, L. E. Kidder, J. Moxon, H. P. Pfeiffer, M. A. Scheel, S. A. Teukolsky, W. Throwe, N. L. Vu, *A Review of Gravitational Memory and BMS Frame Fixing in Numerical Relativity*, [arXiv:2405.08868](https://arxiv.org/abs/2405.08868). See the references in this article for a chronological history of the memory effect.

- [49] D. Cevik, M. Gadella, S. Kuru and J. Negro, Phys. Letts. **A380**,1600 (2016).
- [50] M. Abramowitz and I. A. Stegun (Ed.), Handbook of Mathematical Functions with Formulas, Graphs and Mathematical Tables, Dover Publications Inc., New York, USA, 1965.